

Use of Reverberation Chambers to Determine the Shielding Effectiveness of Physically Small, Electrically Large Enclosures and Cavities

Christopher L. Holloway, *Senior Member, IEEE*, David A. Hill, *Life Fellow, IEEE*, Marco Sandroni, John M. Ladbury, Jason Coder, *Student Member, IEEE*, Galen Koepke, *Member, IEEE*, Andrew C. Marvin, *Senior Member, IEEE*, and Yuhui He

Abstract—With the proliferation of small electric devices in recent years, along with various other applications, there is a growing need to test and determine the shielding properties or shielding effectiveness (SE) of physically small (but electrically large) enclosures or cavities. In this paper, we discuss how a reverberation chamber technique can be used to measure the SE of such enclosures. The approach consists of placing the small enclosure inside a reverberation chamber and using frequency stirring to excite the reverberation chamber. A small surface probe (i.e., a monopole) is mounted on the inside wall of the small enclosure to measure the power level inside the small enclosure. We present measured data from various other reverberation chamber approaches obtained from various enclosure configurations. The data from these other reverberation chamber approaches are used to validate the proposed approach. We also compared measured data to theoretical calculations of the SE for two small enclosures with circular apertures. These various comparisons illustrate that the proposed technique is a valid approach for determining the SE of physically small (i.e., cubic enclosure dimensions of the order of 0.1 m and smaller), but electrically large enclosures (that support several modes at the lowest frequency of interest).

Index Terms—Circular apertures, reverberation chamber, shielding effectiveness (SE), small cavities, small enclosure.

I. INTRODUCTION

FOR MANY applications, shielding enclosures are used to either protect or control immunity and/or emission of electronic devices. In recent years, we have seen these electronic devices becoming smaller, and as a result the need for smaller enclosures (i.e., 0.1 m³ and smaller). There is a need to develop measurement techniques for determining the shielding effectiveness (SE) of these small enclosures.

There presently exists an IEEE standard for measuring the effectiveness of electromagnetic shielding enclosures [1].

Manuscript received February 25, 2008; revised April 28, 2008. Current version published November 20, 2008.

C. L. Holloway, D. A. Hill, J. M. Ladbury, J. Coder, and G. Koepke are with the Electromagnetics Division, National Institute of Standards and Technology (NIST), U.S. Department of Commerce Boulder Laboratories, Boulder, CO 80305 USA (e-mail: holloway@boulder.nist.gov).

M. Sandroni is with the Electromagnetics Division, National Institute of Standards and Technology (NIST), U.S. Department of Commerce Boulder Laboratories, Boulder, CO 80305 USA, and also with the Department of Electrical Engineering, University of Rome “La Sapienza,” Rome 00184, Italy.

A. C. Marvin and Y. He are with the Department of Electronics, University of York, York YO10 5DD, U.K.

Color versions of one or more of the figures in this paper are available online at <http://ieeexplore.ieee.org>.

Digital Object Identifier 10.1109/TEMC.2008.2004580

However, this standard is for room-size enclosures, and as such, the method presented in [1] is not applicable for small-size enclosures or cavities. As a result, the IEEE 299 standard [1] on shielding of large enclosures is currently being modified for these small enclosures. An IEEE 299 Working Group has been formed to investigate different test methods for obtaining SE for smaller enclosures. Enclosures of this size basically fall into two categories: electrically small and electrically large enclosures (electrically large refers to an enclosure that supports several modes at the lowest frequency of interest). This working group will focus on both these categories. However, one of the first tasks of this working group is to concentrate on the latter category, i.e., physically small, but electrically large enclosures. This paper will focus on this latter category and present a technique for determining the SE of physically small, but electrically large enclosures.

By electrically large, we mean that the enclosure dimensions are significantly larger than a free-space wavelength. Experience has shown that a factor of 2 is sufficient. An equivalent requirement is that the mode density is sufficiently high. This point is discussed in more detail in Section VI.

One method for defining the SE of enclosures is the following:

$$SE = -10\log_{10} \left(\frac{P_{in}}{P_{out}} \right) \quad (1)$$

where P_{in} and P_{out} are the power levels inside and outside the enclosure. Measuring the SE of small enclosures poses various problems. The first problem is associated with the internal resonances of the enclosure. This problem occurs when measuring the SE of any size enclosure, both large and small. Because of the resonant nature of the fields inside a shielding enclosure, the fields have an internal modal structure, and as a result, measurement of the fields inside the enclosure is a function of the location where the measurement is performed. For large enclosures, two basic approaches are used to overcome this issue. One approach is to sample the field at various locations in the enclosure, and then take some type of average value of the power level inside. This is basically the approach taken in [1]. However, this is not practical for “truly” physically small enclosures because moving a probe throughout the volume of a small enclosure is problematic. The second approach is based on a nested reverberation chamber technique [2], which is typically done with mode stirring. However, placing a small probe in the center of the small enclosure, as is done in [2], poses difficulties.

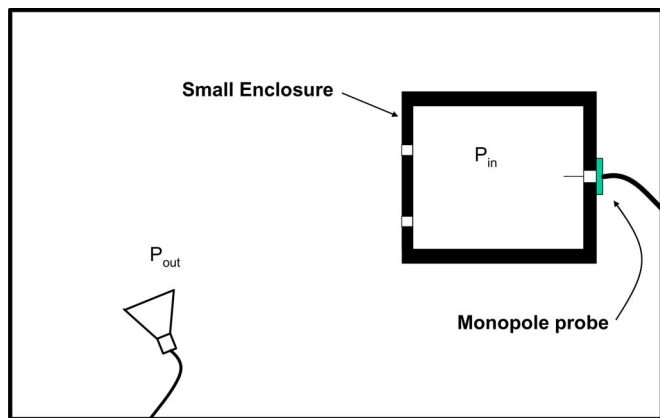


Fig. 1. Illustration of the proposed frequency-stirred reverberation chamber technique.

On the other hand, the use of conventional paddle mode stirring in a small enclosure would also be problematic, i.e., in most applications of measuring small enclosures, it may not be possible to place a small mechanical stirrer inside the enclosures.

In order to overcome these issues, we propose the use of a frequency-stirred reverberation chamber. In this approach, we assume that the enclosure is physically small, but electrically large. A diagram of the proposed approach is shown in Fig. 1. The basic idea is to place the small enclosure in a reverberation chamber. This type of configuration is essentially a nested reverberation chamber [2]. In this setup, the source is placed in the large reverberation chamber. The source is then scanned over a given frequency range. Since some portion of the energy in the outer chamber will couple into the small enclosure, this causes frequency stirring in the small enclosure. As a result, all points in the small enclosure statistically have the same field levels for the data averaged over some bandwidth of frequencies [3]. Hence, the problem of sampling location is resolved without the need to have a paddle (or stirrer) in the small enclosure. The power levels in the small enclosure are monitored by a small monopole probe placed on one of the small enclosure walls. Hill [4] has shown that the normal component of the E -field at the surface of a wall in a well-stirred cavity has the same statistics as a probe placed anywhere in the cavity. Thus, as long as the small enclosure is well stirred (through frequency stirring), a small monopole probe placed on the wall will give the average power level inside the small enclosure. This frequency stirring in the outer chamber can be done with or without a conventional mechanical stirring processor in the large outer reverberation chamber. Use of a combination of both frequency and mechanical stirring in the large outer chamber will lower the uncertainties in the measurements.

While others have used monopole probes throughout an enclosure to monitor the power inside the cavity [5], we suggest an approach where the probe needs to be mounted to only one point on the wall. While we first briefly discussed this proposed approach in [6], in this paper, we discuss the details, and theoretical aspects and rationale for the approach, as well as present various theoretical and experimental results to validate the proposed technique. Building on the results in [6], Greco

and Sarto [7] briefly discuss this approach and present some numerical data.

This paper is organized as follows: after Section I, Section II presents the theory to justify that measurement of the power density in an enclosure with a wall-mounted monopole is equivalent to the power density in the center of the enclosure. Section III presents various other reverberation chamber approaches for determining the SE of the enclosures. These other approaches are needed to validate the proposed approach. In Section IV, the experimental setup used in this paper is discussed. This section also discusses the impedance mismatch correction needed for small monopoles. Section V presents experimental and theoretical results to illustrate the validity of the proposed approach. In this section, we present comparisons to three other reverberation approaches, as well as comparisons to theoretical calculations of the SE for two different small enclosures with circular apertures. We also show that the proposed technique is independent of the probe position (independent of the wall on which the probe is mounted) and independent of the monopole length. In Section VI, we briefly discuss a few points that needed to be addressed when frequency stirring or averaging is used. Section VII summarizes the research presented here and discusses future work.

II. POWER DENSITIES FROM WALL-MOUNTED MONOPOLES: MEASUREMENTS NEAR AND FAR FROM CHAMBER WALLS

In this section, we discuss the rationale for using a wall-mounted monopole, and show that power in an enclosure can be measured either in the center of the enclosure or at the wall of an enclosure. At sufficient distances from the walls, stirrer(s), and source(s) in a reverberation chamber, the ensemble average (over stirrer position or frequency) of the squared magnitude of the electric field is ideally independent of position. This property of statistical uniformity and other field properties can be derived from a plane-wave integral representation with random coefficients with appropriate statistical properties of the fields [8]. In this analysis, it is assumed that the field components are Gaussian random variables with zero means. Statistical uniformity has been verified experimentally with an array of field probes [9], [10]. In this analysis, we will denote the mean-square electric field as E_0^2 . In this environment, the average power received by an antenna is independent of position and orientation, and can be written as [8]

$$\langle P_r \rangle = \frac{1}{2} \frac{E_0^2}{\eta} \frac{\lambda^2}{4\pi} \quad (2)$$

where η is the free-space impedance and λ is the free-space wavelength. The physical interpretation of (2) is that the average received power is the product of the average scalar power density E_0^2/η times the effective area $\lambda^2/4\pi$ of an isotropic antenna times a polarization mismatch factor of 1/2 [11]. When necessary, antenna efficiency and impedance mismatch [8], [11] can also be included in (2). Equation (2) and the following analysis apply to either the reverberation chamber or the shielded enclosure that must also be electrically large. In the reverberation chamber, the source is a transmitting antenna, and in the

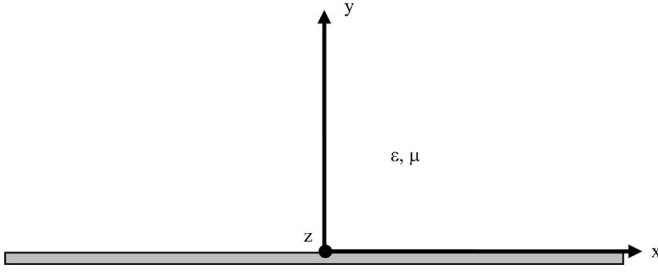


Fig. 2. Single planar wall in a reverberation chamber.

shielded enclosure, the source is leakage. However, the source does not affect the analysis because we are dealing with stirred fields.

A. Field Behavior Near a Wall

Before proceeding to received power, it is instructive to analyze the fields that will illuminate the receiving antenna. Fields in rectangular reverberation chambers have been analyzed for locations near a single wall (planar interface), two walls (right-angle bend), or three walls (right-angle corner) [4]. For practical applications with a monopole probe penetrating a chamber wall, the normal electric field far from the other chamber walls is of most interest. Hence, we can treat the case of a single planar interface shown in Fig. 2. We assume that the wall is perfectly conducting since we are interested only in the field distribution and not the wall losses, as in a calculation of chamber Q [12]. This allows us to use exact image theory in calculating the reflected fields.

The incident electric field \mathbf{E}^i at location \mathbf{r} follows the plane-wave integral form for the total electric field in the free space [8], except for the integration limits

$$\mathbf{E}^i(\mathbf{r}) = \iint_{2\pi} \mathbf{F}(\Omega) \exp(i\mathbf{k}^i \cdot \mathbf{r}) d\Omega \quad (3)$$

where the solid angle Ω is shorthand for the elevation and azimuth angles α and β and $d\Omega = \sin \alpha d\alpha d\beta$. The $\exp(-i\omega t)$ time dependence is suppressed. The integral over solid angle 2π steradians in (3) actually represents the following double integral:

$$\iint_{2\pi} \square d\Omega = \int_{\beta=0}^{\pi} \int_{\alpha=0}^{\pi} \square \sin \alpha d\alpha d\beta \quad (4)$$

The range of β is from 0 to π rather than 0 to 2π because the incident field includes only plane waves propagating toward the interface. The incident vector wavenumber \mathbf{k}^i is

$$\mathbf{k}^i = -k(\hat{\mathbf{x}} \sin \alpha \cos \beta + \hat{\mathbf{y}} \sin \alpha \sin \beta + \hat{\mathbf{z}} \cos \alpha) \quad (5)$$

where the scalar wavenumber $k = 2\pi/\lambda$. The vector angular spectrum $\mathbf{F}(\Omega)$ can be written

$$\mathbf{F}(\Omega) = \hat{\alpha} F_{\alpha}(\Omega) + \hat{\beta} F_{\beta}(\Omega) \quad (6)$$

where $\hat{\alpha}$ and $\hat{\beta}$ are unit vectors that are orthogonal both to each other and to \mathbf{k}^i . To represent a well-stirred field, F_{α} and F_{β}

are taken to be random variables whose statistical properties are given in [8].

The derivations of the average values of the square of the rectangular electric field components $\langle |\mathbf{E}_x^t|^2 \rangle$, $\langle |\mathbf{E}_y^t|^2 \rangle$, and $\langle |\mathbf{E}_z^t|^2 \rangle$, where $\langle \rangle$ represents the average value obtained by stirring, are given in [4]. Here, we utilize only the results for the normal components \mathbf{E}_y^t of the total (incident plus reflected) electrical field because that is the component that excites a wall-mounted monopole. The relevant results from [4] is

$$\langle |\mathbf{E}_y^t(x, y, z)|^2 \rangle = \frac{E_0^2}{3} [1 + \rho_l(2y)] \quad (7)$$

where the longitudinal correlation function ρ_l is [13]

$$\rho_l(2y) = \frac{3}{(2ky)^2} \left[\frac{\sin(2ky)}{2ky} - \cos(2ky) \right] \quad (8)$$

Equation (8) agrees exactly with Dunn's result [14]. The result is independent of x and z . The practical significance of this is that a wall-mounted monopole antenna can be positioned anywhere as long as it is not close to another wall.

The limits of (7) are of practical importance. The limit for large ky is

$$\lim \langle |\mathbf{E}_y^t(x, y, z)|^2 \rangle = \frac{E_0^2}{3}, \quad \text{for } ky \rightarrow \infty. \quad (9)$$

This is the known result for a uniform, well-stirred field component far from chamber walls [8]. At the wall boundary ($y = 0$), (7) reduces to

$$\langle |\mathbf{E}_y^t(x, 0, z)|^2 \rangle = \frac{2E_0^2}{3}. \quad (10)$$

Thus, the mean-square value of the normal component of the electric field is twice that of the value far from the chamber wall.

B. Received Power by Dipole and Monopole Antennas

The purpose of this section is to show that a wall-mounted monopole and a dipole distant from chamber walls receive the same power. The case of a linear dipole antenna has been treated [15], and we will summarize the results here. The sinusoidal approximation for the current $I(y)$ when the transmitting dipole is oriented in the y -direction and centered at $y = y_c$ is [16]

$$I(y) = I_0 \frac{\sin k(H - |y - y_c|)}{\sin kH} \quad (11)$$

where I_0 is the current at the center of the dipole and H is the half-length of the dipole. Equation (11) is an adequate approximation for $H < \lambda/2$. When the dipole is receiving, the open-circuit voltage V_{oc} can be determined by the induced EMF method [16]

$$V_{oc} = -\frac{1}{I_0} \int_{y_c-H}^{y_c+H} E_y^i(y') I(y') dy' \quad (12)$$

Since we assume that the dipole is far from chamber walls, the incident field E_y^i takes the plane-wave integral form over 4π steradians [15] rather than 2π steradians, as in (3).

When the dipole is terminated with a matched load $Z_L = Z_d^*$, where Z_d is the dipole impedance, the average value of the received power can be written as

$$\langle P_r \rangle = \frac{\langle |V_{oc}|^2 \rangle}{4R_d} \quad (13)$$

where $R_d = \text{Re}(Z_d)$ is the input resistance of the dipole. The average of the square of the open-circuit voltage can be derived from (12):

$$\langle |V_{oc}|^2 \rangle = \frac{1}{I_0^2} \int_{y_c-H}^{y_c+H} \int_{y_c-H}^{y_c+H} \langle E_y^i(y_1) E_y^{i*}(y_2) \rangle I(y_1) I(y_2) dy_1 dy_2. \quad (14)$$

The longitudinal correlation function can be used to evaluate the expectation in the integrand in (14) so that (13) can be written as

$$\langle P_r \rangle = \frac{E_0^2}{12R_d I_0^2} \int_{y_c-H}^{y_c+H} \int_{y_c-H}^{y_c+H} \rho_l(y_2 - y_1) I(y_1) I(y_2) dy_1 dy_2. \quad (15)$$

Because of the form of ρ_l in (8), the double integral in (15) is proportional to the input resistance of a linear dipole [15]

$$\int_{y_c-H}^{y_c+H} \int_{y_c-H}^{y_c+H} \rho_l(y_2 - y_1) I(y_1) I(y_2) dy_1 dy_2 = \frac{6\pi I_0^2 R_d}{k^2 \eta}. \quad (16)$$

The radiation resistance R_d can be expressed in terms of standard integrals [15], [16]. Substitution of (16) into (15) yields the same result as (2). This is the expected result since (2) is valid for general antennas, but it is useful to derive the result for a linear dipole by the induced electromotive force (EMF) method because it sets the stage for analysis of the related case of a wall-mounted monopole antenna.

Consider a y -directed monopole of length H fed at the planar wall ($y = 0$) shown in Figs. 2 and 3(a). When the monopole is transmitting, the sinusoidal current approximation is the same as that for the isolated dipole in (11), except that $y_c = 0$ and the current exists only for positive y

$$I(y) = I_0 \frac{\sin k(H-y)}{\sin kH}, \quad 0 < y < H. \quad (17)$$

In a manner similar to (12), we can write the open-circuit voltage using the induced EMF method [16]

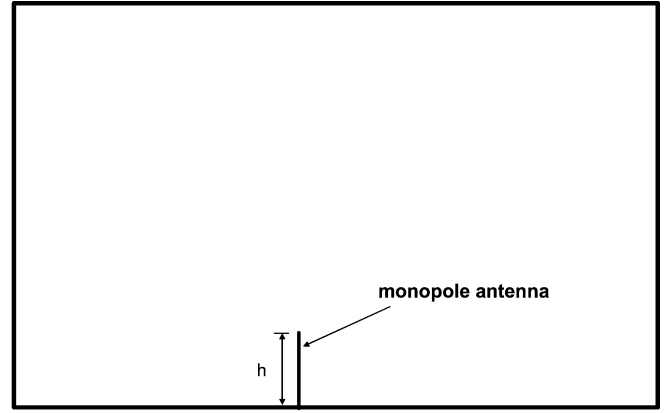
$$V_{oc} = -\frac{1}{I_0} \int_0^H E_y^t(y') I(y') dy'. \quad (18)$$

The total electric field E_y^t in (18) can be written as the sum of the incident field and its image [4]

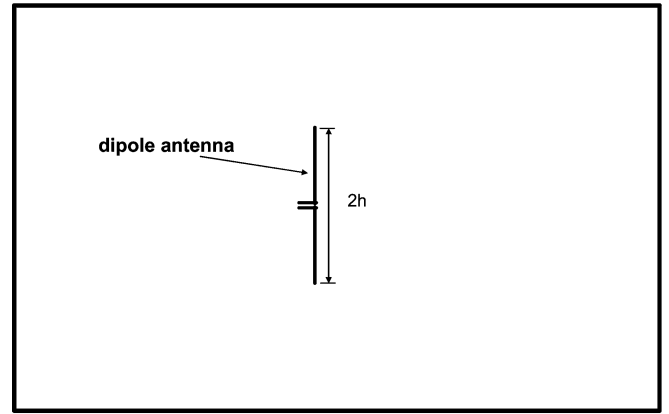
$$E_y^t(y') = E_y^i(y') + E_y^i(-y'). \quad (19)$$

When the monopole is terminated with a matched load $Z_L = Z_m^*$, where Z_m is the monopole impedance, the average value of the received power can be written as

$$\langle P_r \rangle = \frac{\langle |V_{oc}|^2 \rangle}{4R_m} = \frac{\langle |V_{oc}|^2 \rangle}{2R_d}. \quad (20)$$



(a)



(b)

Fig. 3. (a) Wall-mounted monopole antenna in a reverberation chamber. (b) Dipole antenna in the working volume of a reverberation chamber.

The right-hand expression in (20) results from the fact that the monopole impedance and resistance equal one-half that of a dipole antenna of length $2H$ [16]

$$Z_m = \frac{Z_d}{2} \text{ and } R_m = \frac{R_d}{2}. \quad (21)$$

The average of the square of the open-circuit voltage can be derived from (18)

$$\langle |V_{oc}|^2 \rangle = \frac{1}{I_0^2} \int_0^H \int_0^H \langle E_y^t(y_1) E_y^{t*}(y_2) \rangle I(y_1) I(y_2) dy_1 dy_2. \quad (22)$$

The longitudinal correlation function can be used to evaluate the expectation in the integrand in (22) so that (20) can be written as

$$\langle P_r \rangle = \frac{E_0^2}{12R_d I_0^2} \int_0^H \int_0^H [\rho_l(y_2 - y_1) + \rho_l(y_2 + y_1)] \times I(y_1) I(y_2) dy_1 dy_2. \quad (23)$$

After considerable algebra, the double integral in (23) can be evaluated, and (23) reduces to the same result for the isolated

dipole (or any other isolated, matched antenna) as given in (2)

$$\langle P_r \rangle = \frac{1}{2} \frac{E_0^2 \lambda^2}{\eta 4\pi}. \quad (24)$$

The result in (24) is important because it shows that a wall-mounted monopole can be used to monitor the field strength in the center of the chamber, which is given in (2). Hence, the receiving antenna configurations in Fig. 3(a) and (b) are equivalent for monitoring the chamber field strength. For a physically small chamber, the wall-mounted monopole is advantageous.

If we analyze the case of an electrically short monopole ($kH \ll 1$), the previous analysis simplifies significantly. Equation (17) reduces to

$$I(y) = I_0 \left(1 - \frac{y}{H}\right), \quad 0 < y < H. \quad (25)$$

Because of the doubling of the mean square of the normal electric field, as shown in (11), the expected value of the square of the open-circuit voltage can be written as

$$\langle |V_{oc}|^2 \rangle = \left(\frac{H}{2}\right)^2 \left(\frac{2E_0^2}{3}\right) = \frac{H^2 E_0^2}{6}. \quad (26)$$

The $H/2$ quantity in (26) is the effective length (half the physical length) of a short monopole. By substituting (26) into (20), we obtain

$$\langle P_r \rangle = \frac{H^2 E_0^2}{12R_d}. \quad (27)$$

For an electrically short dipole, the radiation resistance is [17]

$$R_d = \frac{2\pi\eta H^2}{3\lambda^2}. \quad (28)$$

If we substitute (28) into (27), we again obtain the expected result for the average received power

$$\langle P_r \rangle = \frac{E_0^2 \lambda^2}{\eta 8\pi}. \quad (29)$$

A similar analysis has been performed for a short dipole antenna [8].

From (2), (24), and (29), we see that the received power is proportional to the mean-square electrical field strength. Hence, the SEs results to follow are applicable to power, electric field strength, and also magnetic field strength since the total field can be represented as an integral of plane waves [8].

If one attempts to use an isolated monopole (for example, the extended center conductor of a coaxial cable), the effectiveness is less clear because it is hard to determine where the antenna starts and the feed ends. (Currents typically are induced on the shield of the coaxial cable.) Such a configuration is shown in Fig. 4(a). If a ground plane is included [as in Fig. 4(b)], then the feed cable is shielded, and the antenna performance is essentially equivalent to any efficient, well-matched antenna. These effects were studied in feeding a microstrip transmission-line radiator [18].

III. OTHER REVERBERATION CHAMBER APPROACHES

In order to illustrate that the proposed frequency stirring approach correlates well with other reverberation chamber ap-

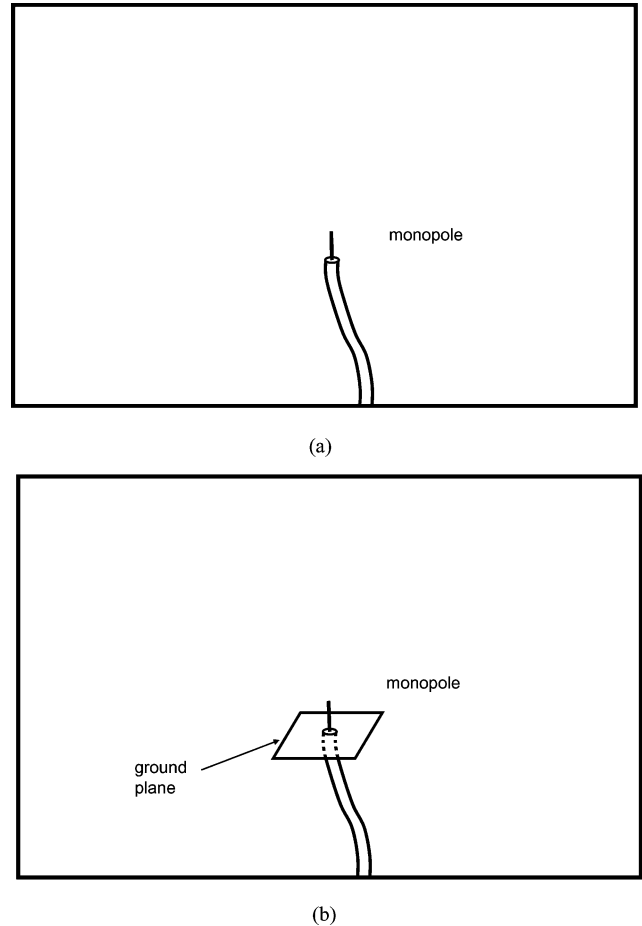


Fig. 4. Monopole antenna in a reverberation chamber. (a) Without ground plane. (b) With ground plane.

proaches, we compare results from this approach to three other reverberation approaches. By comparing to these other three approaches, we investigate two issues: 1) the utility of the frequency stirring and 2) the effectiveness of a surface-based (or wall-mounted) measurement of the power level as compared to a power measurement made in the center of the small chamber. The three other approaches used in this investigation are as follows.

A. Mode Stirred With a Horn Antenna

In this approach, both the large and small reverberation chambers use conventional paddle mode stirring (i.e., paddles in both the two chambers are rotated). A horn antenna is used in the large chamber, and another one is placed in the small chamber to measure the received power.

B. Mode Stirred With a Monopole Antenna

In this approach, both the large and small reverberation chambers use conventional paddle mode stirring. A horn antenna is used in the large chamber, and a monopole probe is placed on one interior wall of the small chamber to measure the received power.

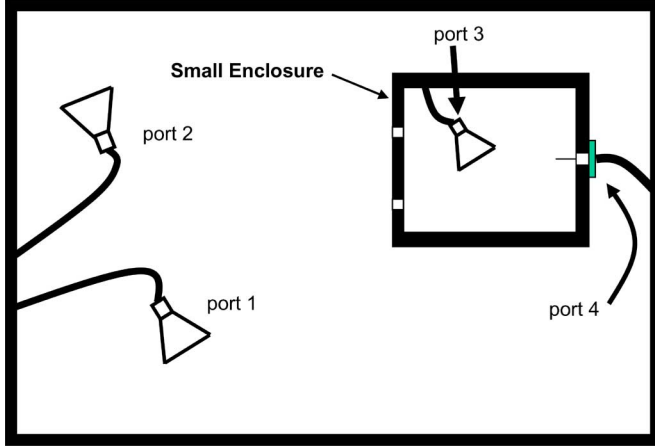


Fig. 5. Experimental setup.

C. Frequency Stirring With a Horn Antenna

In this approach, frequency stirring is performed in the larger chamber. A horn antenna is used in the large chamber, and another one is placed in the small chamber to measure the received power level.

In this comparison, we have chosen two different small enclosures that were large enough to make measurements of these different approaches possible. The first smaller enclosure used in this study is the National Institute of Standards and Technology (NIST) small portable reverberation chamber that has dimensions of 1.49 m × 1.16 m × 1.45 m. This small chamber was placed in the NIST's large chamber. The large chamber has dimensions of 4.60 m × 3.04 m × 2.76 m. Both NIST's small and large chambers have paddles that allow conventional paddle mode stirring. The second smaller enclosure used a portable chamber that has dimensions 0.6 m by 0.7 m by 0.8 m. This small chamber was placed in the large reverberation chamber measuring 4.6 m × 3.0 m × 2.2 m at the University of York. Both University of York's small and large chambers have paddles that allow conventional paddle mode stirring. By comparing these three approaches to the proposed approach (i.e., frequency stirring with a monopole antenna) in the two independent measurement facilities (i.e., at NIST and the University of York), we investigate whether the approach is valid for measuring the SE of a physically small, but electrically large enclosure.

We also validate the proposed approach by comparing measured data to theoretical calculations of the SE for two small enclosures with circular apertures. The theoretical calculations are discussed in Section V-B.

IV. EXPERIMENT METHOD AND SETUP

The measurement setup is shown in Fig. 5. All measurements were performed with a multiport vector network analyzer (VNA) with port 1 connected to a transmitting horn in the outer chamber, port 2 connected to a receiving horn in the outer chamber, port 3 connected to a receiving horn in the inner chamber (the small enclosure), and port 4 connected to a monopole antenna in the inner chamber. The VNA was used as three separate two-port

VNAs with calibrations between ports 1 and 2, 1 and 3, and 1 and 4. With these different S -parameters, the SE as defined in (1) can be obtained for the different reverberation chamber approaches, as discussed in Section V-A. A similar setup was used for the measurements performed at the University of York.

A. Impedance Mismatch Corrections

One has to be careful with antenna impedance mismatch issues when using small monopole antennas. In typical reverberation chamber applications, individuals use antennas that are well matched over the frequency range of interest. However, if small monopole antennas are used, then large reflections at the antenna terminals can occur due to the poor impedance match of the small monopole antenna to the transmission line used to deliver power to the antenna terminals. In order to obtain consistent results, the reflections due to mismatch must be corrected. The correction is explained by noting that the mismatches associated with the monopole antenna will result in measurements of $\langle |S_{41}|^2 \rangle$ being appreciably lower than measurements of $\langle |S_{31}|^2 \rangle$, the port when a well-matched antenna is used. Equivalently, given the same power transmitted through the antenna on port 1, the power received by the monopole will be less than the power coupled to a well-matched receiving antenna on port 3. To correct for this, we applied a mismatch correction to estimate the power that would have coupled to the monopole had it been well matched. If the coupling C_{41} to the monopole is $\langle |S_{41}|^2 \rangle$, then the corrected coupling \tilde{C}_{41} is given as

$$\tilde{C}_{41} = \frac{\langle |S_{41}|^2 \rangle}{1 - |S_{44}|^2} \quad (30)$$

where S_{44} is the free-space reflection coefficient of the monopole. We estimated $|S_{44}|^2$ from our reverberation chamber measurements as $\langle |S_{44}|^2 \rangle$.

With these measured S -parameters, the SE for the four different reverberation techniques is given by one of the following two quantities:

$$SE_{\text{horn}} = \frac{\langle |S_{31}|^2 \rangle}{\langle |S_{21}|^2 \rangle} \quad (31)$$

$$SE_{\text{monopole}} = \frac{\tilde{C}_{41}}{\langle |S_{21}|^2 \rangle} \quad (32)$$

for either the horn or monopole antenna used in the small enclosure (or chamber).

We could also apply impedance mismatch corrections to the antenna at port 2 (the antenna used to monitor the power outside the small enclosure) as well to the horn inside the small enclosure. In general, if we apply corrections to the antennas at ports 2, 3, and 4, the SE can be expressed as one of the following:

$$SE_{\text{horn-horn}} = \frac{\langle |S_{31}|^2 \rangle}{\langle |S_{21}|^2 \rangle} \frac{1 - \langle |S_{22}| \rangle^2}{1 - \langle |S_{33}| \rangle^2}$$

or

$$SE_{\text{horn-monopole}} = \frac{\langle |S_{41}|^2 \rangle}{\langle |S_{21}|^2 \rangle} \frac{1 - \langle |S_{22}| \rangle^2}{1 - \langle |S_{44}| \rangle^2}. \quad (33)$$

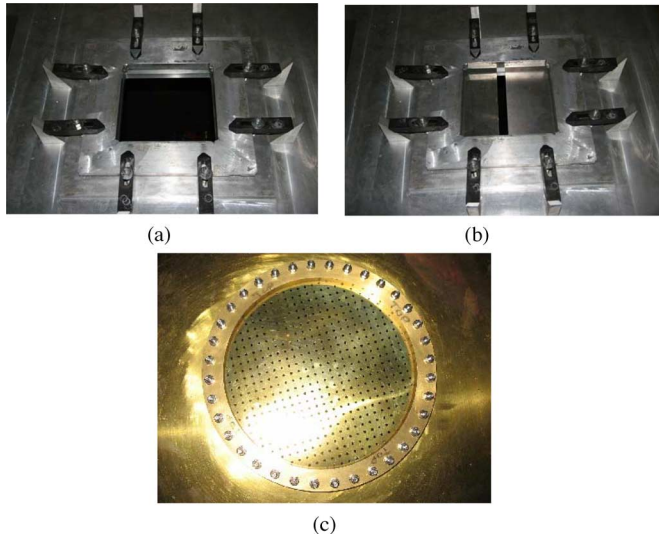


Fig. 6. Illustration of the different apertures used in the two slots for small enclosures. (a) Open aperture used in the NIST small enclosure. (b) Narrow slot used in the NIST small enclosure. (c) Circular hole-grid aperture used in the University of York enclosure.

The second term in these expressions is required for correction of antenna mismatch issues. Note that, in general, when the correction due to S_{33} or S_{44} is not used, an underestimate of SE results. On the other hand, when the correction due to S_{22} is not used, an overestimate of SE results. This correction term approaches a value of 1 for well-matched antennas. As discussed next, the use of small monopole antennas in the small enclosure requires the correction term in the denominator. However, since one typically uses well-matched antenna in the outer reverberation chamber, the numerator is approximately 1.

A monopole antenna could also be used in the outer reverberation chamber to measure the power levels. This monopole could either be mounted on the wall of the outer reverberation chamber or it could be connected to the cable at antenna port 2 shown in Fig. 5. If the monopole is connected to the cable at port 2, care is needed to ensure that currents do not flow on the cable; see discussions at the end of Section II-B. When a monopole is used in the outer reverberation chamber, the mismatch correction in the second expression in (33) is still required. In general, even if the two monopole antennas are identical (the one on the outer chamber and the one on the wall on the small enclosure), $S_{22} \neq S_{44}$. This is because the small enclosure can influence the input impedance of the antenna at port 4, and in turn, cause S_{44} to be different from S_{22} , even though the same monopole antenna is used at both locations.

A correction for the antenna at port 1 is not required because it would cancel since SE is a ratio of two S-parameters referred to port 1. With this stated, it is good practice and highly recommended that a well-matched antenna (for the frequency range of interest) be used as the source antenna (port 1) in the outer reverberation chamber.

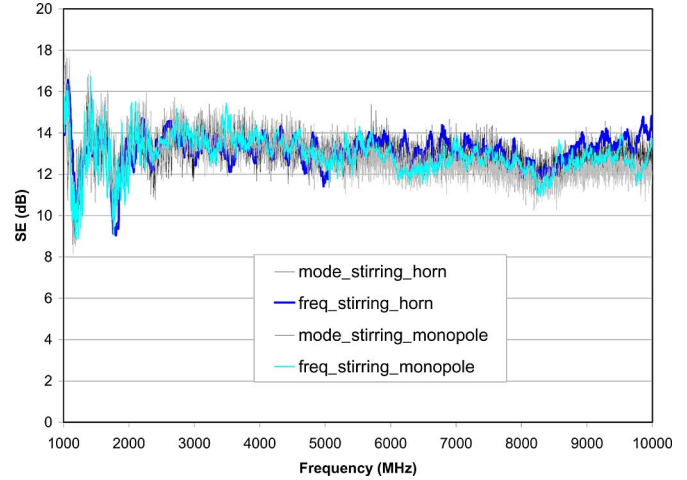


Fig. 7. SE obtained from the four different reverberation chamber approaches for the narrow-slot aperture.

V. VALIDATION OF TECHNIQUE

In this section, we present comparisons to three other reverberation chamber approaches, as well as comparisons to theoretical calculations of the SE for two different small enclosures with circular apertures.

A. Comparison of Four Reverberation Approaches

NIST's small chamber has an aperture (square with a side length of 25.4 cm) in which different panels could be inserted. Thus, besides comparing the four different approaches, we also measured different shielding characteristics of the small enclosure. In this study, we performed measurements with two different panels in the aperture. The two different apertures used here are shown in Fig. 6(a) and (b). These two apertures have different shielding properties. Fig. 7 shows the SE for the narrow slot aperture [see Fig. 6(b)] obtained from all four of the reverberation chamber approaches. The results in this figure (as well as the sequential figure) are labeled as follows. 1) Paddle mode stirring with the horn antenna in the small enclosure is labeled as "mode_stirring_horn." 2) The paddle mode stirring approach with the monopole antenna in the small enclosure is labeled as "mode_stirring_monopole." 3) Frequency stirring with the horn antenna in the small enclosure is labeled as "freq_stirring_horn." 4) Frequency stirring with the monopole antenna is labeled as "freq_stirring_monopole." The impedance mismatch correction was used for the monopole SE results. From this comparison, we see that all four approaches give similar results for the SE of the small enclosure, approximately 13 dB. Fig. 8 shows the SE for the open aperture shown in Fig. 4(a). This figure also compares all four of the reverberation chamber results. Once again, we see from this figure that all four approaches give approximately the same value of the SE for the small enclosure for different enclosure characteristics (i.e., different apertures).

While it is true that the unused antenna loads the chamber, this loading is negligible when compared to the loading of the wall losses of the chamber, and will not affect the comparison.

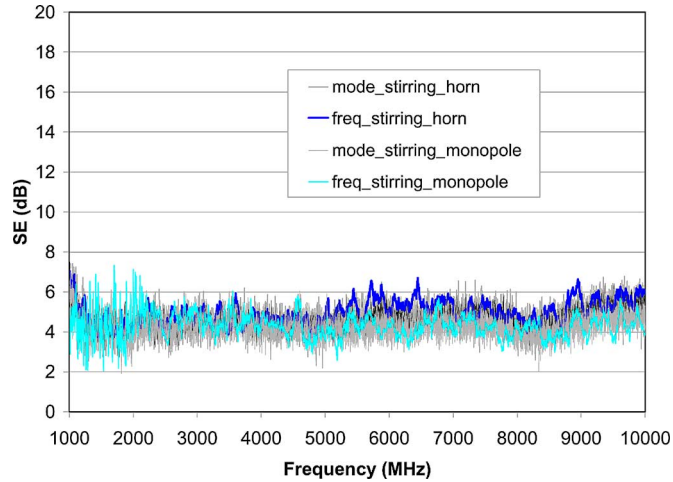


Fig. 8. SE obtained from the four different reverberation chamber approaches for the open aperture.

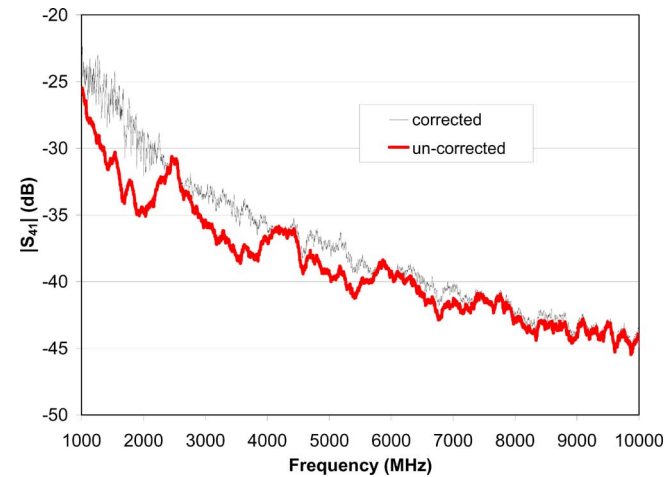


Fig. 9. Comparison of $|S_{41}|$ obtained for the monopole antenna with and without the mismatch corrections.

However, for an actual SE test, the chamber configuration should correspond to the conditions in which it will actually be used. At that point, all loading and Q effects will automatically be taken into account. This is, in contrast to, the measurement of shielding materials in [2], where the SE of material samples in an aperture were intentionally separated from the effects of the chamber Q and aperture size.

As discussed earlier, a correction is needed for the monopole antenna measurements due to the impedance mismatch of the small monopole. The effect of not using this correction is shown in Fig. 9. This figure shows $|S_{41}|$ obtained with and without the correction. These results were obtained from the frequency stirring approach with the monopole antenna. The data without the correction show an oscillation as a function of frequency. This oscillation is associated with the classical resonances seen in the input impedance of linear antennas. The oscillation is not present when the correction is applied, and the resulting SE correlates well with those SE obtained with the horn (see Fig. 7).

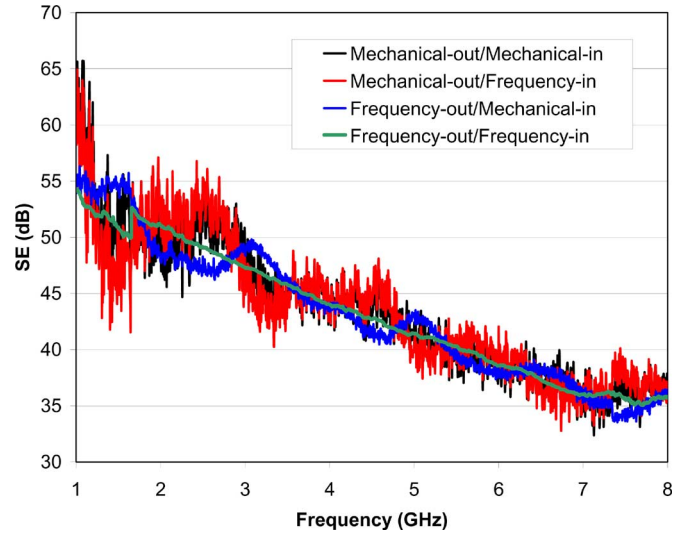


Fig. 10. SE obtained from the four different reverberation chamber approaches for the aperture consisting of the grid of holes.

Measurements were also performed at the University of York's small enclosure. This small enclosure had a circular aperture, and the aperture was filled with a panel that had 3 mm holes on a 10 mm grid [see Fig. 6(c)]. Fig. 10 shows the measured SE from the four different approaches. In these measurements, a monopole was used in the small enclosure, and the four different approaches correspond to different combinations of frequency stirring and mechanical stirring (see figure legend). From this comparison, we see that all four approaches give similar results for the SE of the small enclosure. The correlation of all four approaches presented in Figs. 7, 8, and 10 illustrates that frequency stirring with a small surface wall-mounted probe gives approximately the same results as the other reverberation chamber approaches, and hence, illustrates that the proposed method is a valid approach for determining SE of small enclosures having different enclosure characteristics.

B. Comparison to Theoretical Calculations

The SE for a small enclosure with a circular aperture placed in a reverberation chamber can be obtained analytically with reverberation chamber theory [19] to give

$$SE = 10 \log_{10} \left(\frac{4\pi V_e}{\langle \sigma_t \rangle \lambda Q} \right) \quad (34)$$

where V_e is the volume of the small enclosure, Q is the total quality factor of the enclosure, and $\langle \sigma_t \rangle$ is the averaged transmission cross section of the aperture. The total quality factor is given by

$$Q^{-1} = Q_{\text{wall}}^{-1} + Q_{\text{aper}}^{-1} + Q_{\text{antenna}}^{-1} \quad (35)$$

where Q_{wall} is associated with the wall loss, Q_{aper} is associated with the aperture leakage, and Q_{antenna} is associated with the

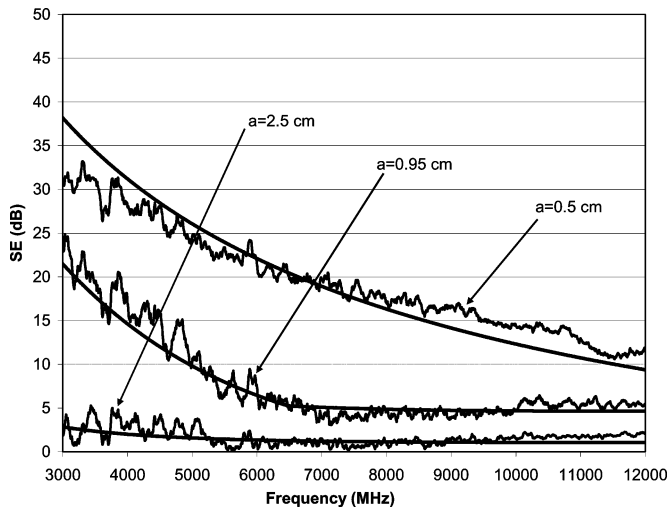


Fig. 11. Comparison of the theory and measured SE for box 1 (15.2, 25.3, and 43.2 cm) for three different circular apertures. The smooth curves correspond to the theoretical predictions.

energy dissipated in the antenna, and are given by

$$Q_{\text{wall}} = \frac{3V_e}{2\mu_r S \delta} \quad Q_{\text{aper}} = \frac{4\pi V_e}{\lambda \langle \sigma_t \rangle} \quad Q_{\text{antenna}} = \frac{16\pi^2 V_e}{\lambda^3} \quad (36)$$

where S is the surface area of the small enclosure, and μ_r and δ are the permeability and skin depth of the enclosure walls. In general, the calculation of the transmission cross section for an arbitrary aperture is involved [20], [21]. However, the circular aperture does not have strong resonances, and for a circular aperture, $\langle \sigma_t \rangle$ can be approximated by [19]

$$\langle \sigma_t \rangle = \frac{16}{9\pi} k^4 a^6, \quad \text{for } ka \leq 1.29$$

$$\langle \sigma_t \rangle = \frac{\pi}{2} a^2, \quad \text{for } ka > 1.29 \quad (37)$$

where a is the radius of the circular aperture.

In order to compare the theoretical calculation to the proposed measurement technique, we constructed two different-size small enclosures out of aluminum (box 1: 15.2 cm \times 25.3 cm \times 43.2 cm and box 2: 15.7 cm \times 12.7 cm \times 22.8 cm). Four circular holes of different sizes were cut into one side of both of the two boxes. The radii a of the four circular apertures were 2.55, 1.9, 0.95, and 0.5 cm. By placing copper tape over three of the holes, the SE for each individual circular aperture could be measured. In these measurements, the same monopole (with length of 1.3 cm) was used to measure the power both outside and inside of the small enclosure. Figs. 11 and 12 compare the theoretical to the measured SE for the two enclosures for three different apertures. The comparisons illustrate that the results from the proposed approach correlate well with the theoretical results. Comparisons for the fourth aperture show similar correlation to theory. This illustrates that the proposed approach is valid for determining the SE of a small enclosure.

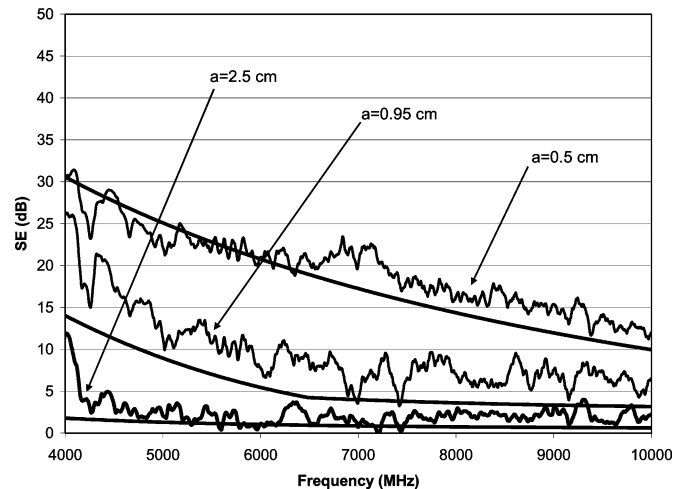


Fig. 12. Comparison of the theory and measured SE for box 2 (15.7, 12.7, and 22.8 cm) for three different circular apertures. The smooth curves correspond to the theoretical predictions.

C. Comparison for Different Probe Positions and Probe Sizes

In order for this proposed technique to be useful, the measured value of SE should be independent of the probe position (i.e., independent of the wall of the small enclosure to which the probe is attached). This is true as long as the probe does not get too close to a corner. If this occurs, the wall-mounted probe does not measure the same power as that measured by a probe placed at the center of the enclosure, and as a result, the accuracy of measured power comes into question. Also, the measured SE should be independent of the size of the monopole probe that is used, as long as the probe is calibrated correctly. This is true only for an electrically short monopole probe. If the monopole probe becomes electrically large ($H \geq \lambda$), then calibrations and impedance mismatch correction will become difficult. In order to show that the technique is independent of the wall on which the probe is mounted, as well as independent of monopole length, measurements were performed in the NIST chamber for a small enclosure with a probe mounted on two different walls and with two different monopole probe lengths (1.3 and 2.5 cm). The small enclosure (15.2, 25.3, and 43.2 cm) had different circular apertures, as discussed earlier. Fig. 13 compares the measured SEs for different probe sizes and positions. The two groups of curves in this figure correspond to different aperture radii. Once again, in these measurements, the same monopole was used to monitor the power both outside and inside the small enclosure. For each aperture size, there are four different results: two of the results correspond to the 1.3 cm probe placed on two different walls, and the other two results correspond to the 2.5 cm probe placed on the same two walls. For these results, we see that the proposed technique is nearly independent of the probe location and probe size.

In order to further illustrate this point, measurements for a second small enclosure (48 cm \times 48 cm \times 12 cm rectangular metal box) were performed in the chamber at the University of York. The front of the box had a number of rectangular slit

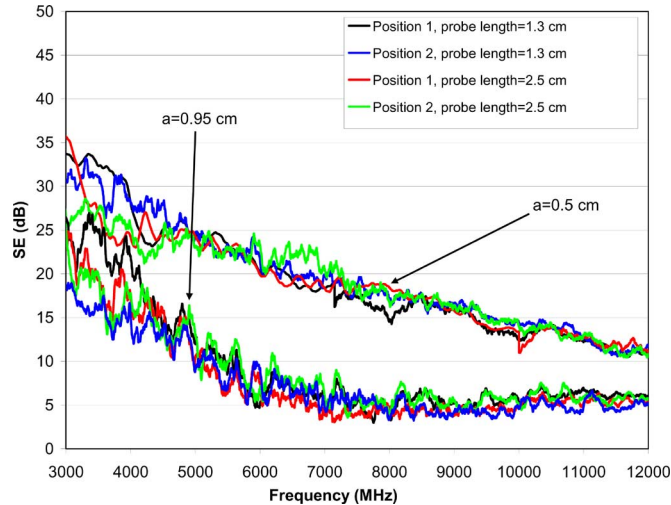


Fig. 13. Comparison of measured SE for two different probe locations and two different probe lengths for measurements made in the NIST chamber for a small enclosure (15.7, 12.7, and 22.8 cm).

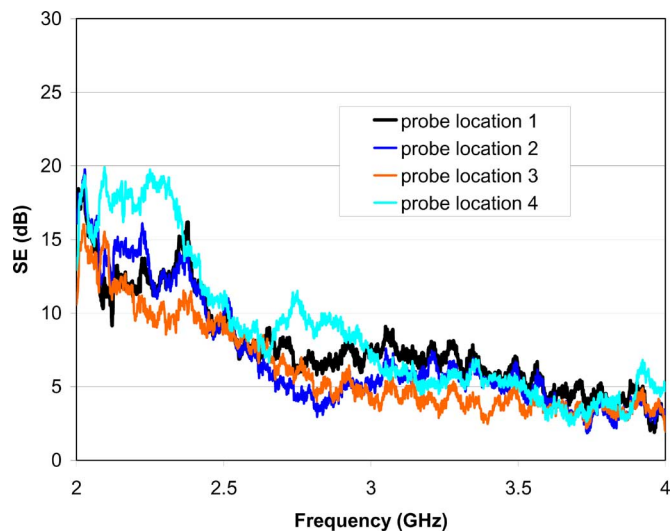


Fig. 14. Comparison of the measured SE for four different probe locations for measurements made in the University of York chamber for a small enclosure (48, 48, and 12 cm).

apertures. Measurements were performed at four different probe mounting positions (two mounting locations were on the top and two locations were on the side of the box). A comparison of the SE for the four positions is given in Fig. 14. Once again, we see good correlation for all four of the measurements. There is some deviation at the low frequency. This deviation is due to low modal density at the lower frequencies end for the size enclosure.

In general, the measurement procedure is independent of the location where the wall-mounted monopole is located. However, a few guidelines should be followed. If only one of these guidelines is not followed, the wall-mounted probe may not measure the same power as that of a probe placed in the center of the enclosure, and the accuracy with which power is measured inside

the small enclosure comes into question. As discussed earlier, the monopole probe should not be placed near a corner of the enclosure. If possible, avoid locating the monopole probe close to any aperture. Also, avoid direct illumination of the monopole probe by an aperture on the wall opposite to that on which the monopole is mounted.

Uncertainties in reverberation chamber measurements, as discussed in this section, are discussed in [2], [10], and [22]. In particular, in [10], it is shown that measurement uncertainties in reverberation chambers are below 1 dB.

VI. COMMENTS ABOUT FREQUENCY STIRRING AND FREQUENCY LIMITS

A few issues with frequency stirring (or averaging) require brief discussion. The one main concern with frequency stirring is what bandwidth (BW) should be used in the frequency averaging process. In choosing this bandwidth, two criteria must be met: 1) one based on a minimum BW and 2) the other based on a maximum BW.

The first criterion is based on a minimum allowable BW. There must be a significant number of modes in the enclosure such that we have independent frequency samples for the chosen averaging bandwidth. The mode density $D(f)$ in the enclosure is approximately [23], [24]

$$D(f) \approx \frac{8\pi V_e f^2}{c^3} \quad (38)$$

where V_e is the enclosure volume and c is the speed of light; so the number of modes in a bandwidth N_{BW} is the product of the mode density times the bandwidth

$$N_{\text{BW}} \approx \frac{8\pi V_e f^2 \text{BW}}{c^3} \quad (39)$$

We need N_{BW} to be much greater than 1 [3]. To achieve this, BW in (39) must satisfy

$$\text{BW} \gg \frac{c^3}{8\pi V_e f^2}. \quad (40)$$

This assumes that BW is somewhat greater than the single-mode bandwidth f/Q , but this is the typical case, since f/Q is generally small for large Q [25].

The second criterion is based on a maximum allowable BW. There are two issues that one needs to be careful with when choosing the maximum BW. The first is associated with the shielding properties of the small enclosure under test. If the bandwidth is too large, then resonances in the actual shielding response of the small enclosure would be smoothed out. The second issue is associated with the outer reverberation chamber. If the BW is too large and the Q of the outer reverberation chamber changes significantly over that BW, then the frequency averaging approach is not valid. If the test environment (the outer reverberation chamber) is changing over this BW (changes due to the change in Q), the samples used for frequency averaging are not associated with the same conditions (i.e., the samples are uncorrelated).

The proposed approach assumes that the enclosure is electrically large, and as such there is a minimum frequency limit in this measurement procedure. In order for the frequency stirring approach to be valid, the enclosure must be able to support at least 60 modes for a given enclosure size and frequency. Thus, the minimum frequency at which this procedure can be used for is a given enclosure size is [23]

$$f_{\min} = c \left(\frac{90}{4\pi} \frac{1}{V_e} \right)^{1/3} \quad (41)$$

where V_e is the volume of the small enclosure.

VII. CONCLUSION AND DISCUSSION

In this paper, we have presented a reverberation chamber technique for measuring the SE of physically small, but electrically large enclosures or cavities. The approach consists of placing the small enclosure inside a large reverberation chamber, and using frequency stirring as a means of averaging in the reverberation chamber. Frequency stirring eliminates the need for paddle stirring in the small enclosure. A small surface probe (i.e., a monopole) is mounted on the inside wall of the small enclosure to measure the power level inside the small enclosure. This frequency stirring in the outer chamber can be done with or without a conventional mechanical stirring processor in the large outer reverberation chamber. Using a combination of both frequency and mechanical stirring in the large outer chamber will lower the uncertainties in the measurements.

In order to validate this approach, we presented data from four different reverberation chamber approaches obtained from various enclosure configurations (different enclosure sizes and different aperture characteristics). We have shown that all four approaches give similar values for the SE of the small enclosure. We also compared measured data to theoretical calculations of the SE for two small enclosures having different sizes of circular apertures. These various comparisons illustrate that frequency stirring with a small surface wall-mounted probe gives similar results as those from other reverberation chamber approaches, and correlates very well with the theoretical calculations. Hence, this illustrates that the proposed technique is valid for determining the SE of physically small (i.e., enclosures of the order 0.1 m^3 and smaller), but electrically large enclosures (that support several modes, at the lowest frequency of interest).

This paper has laid out the framework, and presented experimental and theoretical evidence to support the possibility of using reverberation chambers for testing SE of small enclosures. There are various issues that need further research and discussion. For example, what bandwidth should be used in frequency stirring or averaging; what is the optimal monopole probe length for a given frequency range; and what type of variations should one expect for low mode density? These and other related topics are presently being investigated, and will be the topics of future publications.

REFERENCES

- [1] *IEEE Standard Method for Measuring the Effectiveness of Electromagnetic Shielding Enclosures*, IEEE Standard 299, 1997.
- [2] C. L. Holloway, D. A. Hill, J. Ladbury, G. Koepke, and R. Garzia, "Shielding effectiveness measurements of materials in nested reverberation chambers," *IEEE Trans. Electromagn. Compat.*, vol. 45, no. 2, pp. 350–356, May 2003.
- [3] D. A. Hill, "Electronic mode stirring for reverberation chambers," *IEEE Trans. Electromagn. Compat.*, vol. 36, no. 4, pp. 294–299, Nov. 1994.
- [4] D. A. Hill, "Boundary fields in reverberation chambers," *IEEE Trans. Electromagn. Compat.*, vol. 47, no. 2, pp. 281–290, May 2005.
- [5] M. Hoijer, "Radiated susceptibility test in reverberation chambers," Swedish Defence Res. Agency, Sweden, Scientific Rep. FOI-R-2007-SE, Jun. 2006.
- [6] C. L. Holloway, J. Ladbury, J. Coder, G. Koepke, and D. A. Hill, "Measuring shielding effectiveness of small enclosures/cavities with a reverberation chamber," in *Proc. IEEE 2007 Int. Symp. Electromagn. Compat.*, Honolulu, HI, 8–13 Jul., pp. 1–5.
- [7] S. Greco and M. S. Sarto, "Hybrid mode-stirring technique for shielding effectiveness measurement of enclosures using reverberation chamber," in *Proc. IEEE 2007 Int. Symp. Electromagn. Compat.*, Honolulu, HI, 8–13 Jul., pp. 1–6.
- [8] D. A. Hill, "Plane wave integral representation for fields in reverberation chambers," *IEEE Trans. Electromagn. Compat.*, vol. 40, no. 3, pp. 209–217, Aug. 1998.
- [9] M. L. Crawford and G. H. Koepke, "Design, evaluation, and use of a reverberation chamber for performing electromagnetic susceptibility/vulnerability measurements," U.S. Nat. Bur. Stand., Washington, DC, Tech. Note 1092, 1986.
- [10] J. Ladbury, G. Koepke, and D. Cammell, "Evaluation of the NASA Langley research center mode-stirred chamber facility," U.S. Natl. Inst. Stand. Technol., Boulder, CO, Tech. Note 1508, 1999.
- [11] C. T. Tai, "On the definition of effective aperture of antennas," *IEEE Trans. Antennas Propag.*, vol. AP-9, no. 2, pp. 224–225, Mar. 1961.
- [12] D. A. Hill, "A reflection coefficient derivation for the Q of a reverberation chamber," *IEEE Trans. Antennas Propag.*, vol. 38, no. 4, pp. 591–592, Nov. 1996.
- [13] D. A. Hill and J. Ladbury, "Spatial-correlation functions of fields and energy density in a reverberation chamber," *IEEE Trans. Electromagn. Compat.*, vol. 44, no. 1, pp. 95–101, Feb. 2002.
- [14] J. M. Dunn, "Local, high-frequency analysis of the fields in a mode-stirred chamber," *IEEE Trans. Electromagn. Compat.*, vol. 32, no. 1, pp. 53–58, Feb. 1990.
- [15] D. A. Hill, "Linear dipole response in a reverberation chamber," *IEEE Trans. Electromagn. Compat.*, vol. 41, no. 4, pp. 365–368, Nov. 1999.
- [16] E. C. Jordan and K. G. Balmain, *Electromagnetic Waves and Radiating Systems*. Englewood Cliffs, NJ: Prentice-Hall, 1968.
- [17] R.F. Harrington, *Time-Harmonic Electromagnetic Fields*. New York: McGraw-Hill, 1961.
- [18] D. A. Hill, D. G. Camell, K. H. Cavcey, and G. H. Koepke, "Radiated emissions and immunity of microstrip transmission lines: Theory and reverberation chamber measurements," *IEEE Trans. Electromagn. Compat.*, vol. 38, no. 2, pp. 165–172, May 1996.
- [19] D. A. Hill, M. T. Ma, A. R. Ondrejka, B. F. Riddle, M. L. Crawford, and R. T. Johnk, "Aperture excitation of electrically large, lossy cavities," *IEEE Trans. Electromagn. Compat.*, vol. 36, no. 3, pp. 169–178, Aug. 1994.
- [20] C. M. Butler, Y. Rahmat-Samii, and R. Mittra, "Electromagnetic penetration through apertures in conducting surface," *IEEE Trans. Antennas Propag.*, vol. AP-26, no. 1, pp. 82–93, Jan. 1978.
- [21] H. Levine and J. Schwinger, "On the theory of electro-magnetic wave diffraction by an aperture in an infinite plane conducting screen," *Commun. Pure Appl. Math.*, vol. 3, pp. 355–391, 1950.
- [22] D. A. Hill and M. Kanda, "Measurement uncertainties of radiated emissions," U.S. Natl. Inst. Stand. Technol., Boulder, CO, Tech. Note 1389, 1997.
- [23] B.-H. Liu, D. C. Chang, and M. T. Ma, "Eigenmodes and the composite quality factor of a reverberating chamber," U.S. Nat. Bur. Stand., Washington, DC, Tech. Note, 1066, 1983.
- [24] D. A. Hill, "Electromagnetic theory of reverberation chambers," U.S. Natl. Inst. Stand. Technol., Boulder, CO, Tech. Note 1506, 1998.
- [25] R. H. Price, H. T. Davis, and E. P. Wenaas, "Determination of the statistical distribution of electromagnetic-field amplitudes in complex cavities," *Phys. Rev. E*, vol. 48, pp. 4716–4729, 1993.



Christopher L. Holloway (S'86–M'92–SM'04) was born in Chattanooga, TN, on March 26, 1962. He received the B.S. degree in engineering from the University of Tennessee at Chattanooga, Chattanooga, in 1986, and the M.S. and Ph.D. degrees from the University of Colorado at Boulder, Boulder, in 1988 and 1992, respectively, both in electrical engineering.

During 1992, he was a Research Scientist with Electro Magnetic Applications, Inc., in Lakewood, CO. His responsibilities included theoretical analysis and finite-difference time-domain modeling of various electromagnetic problems. From 1992 to 1994, he was with the National Center for Atmospheric Research (NCAR), Boulder, where he was engaged in wave propagation modeling, signal processing studies, and radar systems design. From 1994 to 2000, he was with the Institute for Telecommunication Sciences (ITS), U.S. Department of Commerce, Boulder, where he was involved in wave propagation studies. Since 2000, he has been with the National Institute of Standards and Technology (NIST), Boulder, where he has been engaged in research on electromagnetic theory. He is also on the Graduate Faculty at the University of Colorado at Boulder. His current research interests include electromagnetic field theory, wave propagation, guided wave structures, remote sensing, numerical methods, and electromagnetic compatibility (EMC)/electromagnetic interference (EMI) issues.

Dr. Holloway is currently serving as the Co-Chair for Commission A of the International Union of Radio Science and is an Associate Editor for the IEEE TRANSACTIONS ON ELECTROMAGNETIC COMPATIBILITY. He was the Chairman for the Technical Committee on Computational Electromagnetics (TC-9) of the IEEE Electromagnetic Compatibility Society from 2000 to 2005, an IEEE Distinguished Lecturer for the EMC Society from 2004 to 2006, and is currently serving as Co-Chair for the Technical Committee on Nanotechnology and Advanced Materials (TC-11) of the IEEE EMC Society. He was the recipient of the 2008 IEEE EMC Society Richard R. Stoddart Award, the 2006 Department of Commerce Bronze Medal for his work on radio wave propagation, the 1999 Department of Commerce Silver Medal for his work on electromagnetic theory, and the 1998 Department of Commerce Bronze Medal for his work on printed circuit boards.



David A. Hill (M'72–SM'76–F'87–LF'08) was born in Cleveland, OH, on April 21, 1942. He received the B.S.E.E. and M.S.E.E. degrees from Ohio University, Athens, in 1964 and 1966, respectively, and the Ph.D. degree in electrical engineering from Ohio State University, Columbus, in 1970.

From 1970 to 1971, he was a Visiting Fellow with the Cooperative Institute for Research in Environmental Sciences, Boulder, CO, where he was engaged in research on pulse propagation. From 1971 to 1982, he was with the Institute for Telecommunica-

tions Sciences, Boulder, where his research involved antennas and propagation. Since 1982, he has been with the National Institute of Standards and Technology, Boulder, where he has been engaged in research on electromagnetic theory. He is also a Professor Adjoint in the Department of Electrical and Computer Engineering, University of Colorado, Boulder.

Prof. Hill is a member of the International Union of Radio Science (URSI) Commissions A, B, E, and F. He was a Technical Editor for the IEEE TRANSACTIONS ON GEOSCIENCE AND REMOTE SENSING and the IEEE TRANSACTIONS ON ANTENNAS AND PROPAGATION.



Marco Sandroni was born in Viterbo, Italy, in 1982. He received the M.S. degree (with honors) in electrical engineering from "La Sapienza" University, Rome, Italy, in July 2007.

He received the University Student Grants in Electronics for three years at the Laboratory of Methods and Measurements, Department of Electric Engineers, "La Sapienza." He attended the Socrates Intensive Program (IP): "ElectroMagnetic Compatibility (EMC) related to Wireless Communication Systems" at "Katholieke Hogeschool Brugge Oostende (KHBO)," Brugge, Belgium. He is currently a Project Engineer with Bombardier Transportation, Istanbul, Turkey, to construct a new metro line.



John M. Ladbury was born in Denver, CO, in 1965. He received the B.S.E.E. and M.S.E.E. degrees in signal processing from the University of Colorado, Boulder, in 1987 and 1992, respectively.

Since 1987, he has been engaged in research on electromagnetic compatibility (EMC) metrology and facilities with the Radio Frequency Technology Division, National Institute of Standards and Technology (NIST), Boulder. His current research interests include reverberation chambers, with some investigations into other EMC-related topics such as time-domain measurements and probe calibrations. He is also involved in the revision of RTCA DO160D.

Mr. Ladbury is a member of the International Electrotechnical Commission (IEC) joint task force on reverberation chambers. He has received three "best paper" awards at IEEE International EMC symposia over the last six years.



Jason Coder (S'05) was born in Ames, IA, on March 21, 1986. He received the B.S.E.E. degree in 2008 from the University of Colorado Denver, Denver. He is currently pursuing the M.S.E.E. degree.

Since 2005, he has been with the RF Fields Group, National Institute of Standards and Technology, Boulder, CO. He holds a U.S. Patent. His current research interests include reverberation chambers, electromagnetic compatibility (EMC) measurements, and their methodologies. Before joining NIST, he worked on several meteorological systems including a wind profiling radar and a unique way of measuring wind

speed and direction.



Galen Koepke (M'89) received the B.S.E.E. degree from the University of Nebraska, Lincoln, NE, in 1973 and the M.S.E.E. from the University of Colorado, Boulder, CO, in 1981.

He is a National Association of Radio and Telecommunications Engineers (NARTE) Certified Electromagnetic Compatibility (EMC) Engineer. He is a Project Leader for the Field Parameters and EMC Applications Program in the RF Fields Group, National Institute of Standards and Technology, Boulder. The goals of this program are to develop

standards and measurement techniques for radiated electromagnetic fields and to apply statistical techniques to complex electromagnetic environments and measurement situations. A cornerstone of this program has been the NIST work on complex cavities, such as the reverberation chamber, aircraft compartments, etc. He has contributed, over the years, to a wide range of electromagnetic issues. His current research interests include measurements and research looking at emissions, immunity, electromagnetic shielding, probe development, antenna and probe calibrations, and generating standard electric and magnetic fields. He is also involved in transverse electromagnetic (TEM) cell, anechoic chamber, open-area-test-site (OATS), and reverberation chamber measurement techniques along with a portion devoted to instrumentation software and probe development.

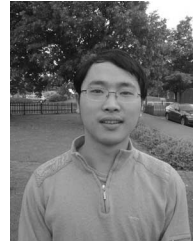


Andrew C. Marvin (M'83–SM'06) received the B.Eng., M.Eng. and Ph.D. degrees in electrical engineering from the University of Sheffield, Sheffield, U.K., between 1972 and 1978.

He is a Professor of Applied Electromagnetics, a Leader of the Physical Layer Research Group, and the Deputy Head of the Department of Electronics, University of York, York, U.K. where he is also the Technical Director of York Electromagnetic Compatibility (EMC) Services Ltd. His current research interests include EMC measurement techniques and

shielding.

Prof. Marvin is a Member of the Institution of Engineering and Technology (IET). He represents the U.K. on International Union of Radio Science (URSI) Commission A (Electromagnetic Metrology). He is a Co-Convenor of the International Special Committee on Radio Interference (CISPR)/International Electrotechnical Commission (IEC) Joint Task Force on the use of Transverse Electromagnetic (TEM) Cells for EMC Measurements, the Vice-Chairman of the IEEE Std-299 Working Group on Shielding Effectiveness Measurement, and an Associate Editor of the IEEE TRANSACTIONS ON ELECTROMAGNETIC COMPATIBILITY.



Yuhui He was born in JiangXi, China, in 1983. He received the B.S.E.E degree in electrical engineering from Dalian University of Technology, Dalian, China, in 2004. He is currently working toward the Ph.D. degree in the Department of Electronics, University of York, York, U.K.

His current research interests include the measurement of electromagnetic shielding of electrically small enclosures and the applications of reverberation chambers.